Enhancing Mechanical Properties of Multiwall Carbon Nanotubes via sp^3 Interwall Bridging

Z. H. Xia,[1] P. R. Guduru,[2] and W. A. Curtin[2]

[1]*Department of Mechanical Engineering, The University of Akron, Akron, Ohio 44325, USA*
[2]*Division of Engineering, Brown University, Providence, Rhode Island 02912, USA*

(Received 15 February 2007; published 14 June 2007)

Molecular dynamics (MD) simulations under transverse shear, uniaxial compression, and pullout loading configurations are reported for multiwall carbon nanotubes (MWCNTs) with different fraction of interwall sp^3 bonds. The interwall shear coupling in MWCNTs is shown to have a strong influence on load transfer and compressive load carrying capacity. A new continuum shear-coupled-shell model is developed to predict MWCNT buckling, which agrees very well with all MD results. This work demonstrates that MWCNTs can be engineered through control of interwall sp^3 coupling to increase load transfer, buckling strength, and energy dissipation by nanotube pullout, all necessary features for good performance of nanocomposites.

DOI: 10.1103/PhysRevLett.98.245501 PACS numbers: 62.25.+g, 46.05.+b, 31.15.Qg

The deformation mechanisms in carbon nanotubes determine their ability to provide high stiffness, strength, toughness, and engineered friction, in advanced structural materials. Although single-wall carbon nanotubes (SWCNTs) have theoretical tensile strengths approaching 100 GPa [1,2], they have several limitations: resistance to compressive loading can be limited due to buckling; the achievable volume fraction is limited by the pore space in the nanotube; and functionalizing to enhance coupling to a matrix can introduce strength-limiting flaws. Multiwall carbon nanotubes (MWCNTs), consisting of nested concentric SWCNTs, might overcome some of these limitations but often do not. In ideal MWCNTs with interwall van der Waals coupling, the buckling behavior is not improved over SWCNTs; load cannot be transferred from the outer wall to the inner walls, and energy dissipation after fracture is small because of easy sliding between walls (''telescoping'') [3–5]. Little research addresses these fundamental limitations of the CNTs and so engineering of CNT-based structural materials to achieve desired performance goals thus requires design of the MWCNT structure itself. There has been some experimental and computational work on modifying the interwall coupling in graphite [4,5] and nanotube ropes [6,7] through controlled sputtering and irradiation. The shear modulus of graphite is increased by an order of magnitude when subjected to neutron irradiation [4], which was attributed to the formation of interlayer sp^3 bonds [5]. Molecular dynamics (MD) modeling of the effect of such irradiation-induced defects in MWCNTs showed that a small number of defects can have a large effect on the interlayer shear strength, improving load transfer to the inner shells [8]. These studies suggest that MWCNTs with optimized mechanical properties can be engineered by creating a controlled density of interwall bridges.

Here, we demonstrate that interwall coupling in MWCNTs via sp^3 bonding can enhance load transfer and increase buckling resistance significantly, permitting full mechanical participation of all walls in a MWCNT. We further show that MWCNT buckling failure computed in molecular dynamics models is consistent with a new ''shear-coupled-shell'' model that bridges the gap between the van der Waals coupling in ideal MWCNTs and a fully-continuum transversely-isotropic shell material. Finally, preliminary results show large enhancements in the pullout forces in MWCNTs due to interwall bonding. This work motivates a new direction for design of MWCNTs for mechanical performance and provides a theoretical framework for analysis of properties versus interwall coupling.

We study the influence of interwall sp^3 bonding on MWCNT mechanical properties by simulating shear, compression, and pullout loading of armchair MWCNTs containing different densities of randomly distributed interwall sp^3 bonds using molecular dynamics (MD). The forces on atoms were calculated using a reactive empirical bond-order potential coupled to a Lennard-Jones (LJ) potential for the interwall coupling [9,10]. A cutoff distance of 20 nm was used in the LJ potential to capture the long-ranged van der Waals potential. The Verlet algorithm with 2 fs time step was used to integrate the equations of motion, with velocity rescaling to maintain a constant temperature of 0.05 K. Samples were generated starting from an ideal MWCNT of the desired length L and diameter d, with $L/d = 2$ fixed for all MWCNTs studied, and adding sp^3 bonds at random locations by incrementally moving two close atoms in adjacent walls from the graphitic wall spacing to the sp^3 bond distance. After adding the desired fraction f of sp^3 bonds, defined as the number of interwall sp^3 bonds divided by the number of atoms in the system, the entire nanotube was relaxed to equilibrium under zero applied load. By our definition, the maximum fraction of sp^3 interwall bonds is $\approx$11.7%, corresponding to a diamondlike structure. Figure 1 shows the relaxed structure of a double-wall CNT containing 6% sp^3 interwall bonds and the local distortions necessary to accommodate the mixed bonding are evident.

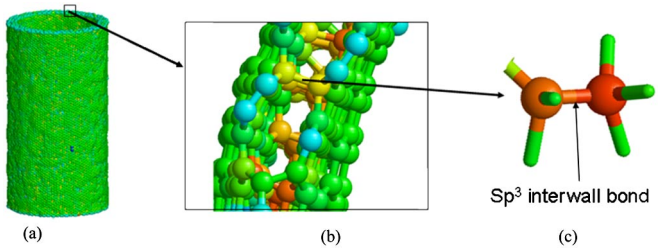

FIG. 1 (color online). Atomic structure of a CNT with interwall sp^3: (a) Initial geometry of a MWCNT with the surface undulations due to the presence of sp^3 bonds, (b) A close-up view of the atomic structure, showing sp^3 bonds bridging the walls and (c) An individual sp^3 interwall bond.

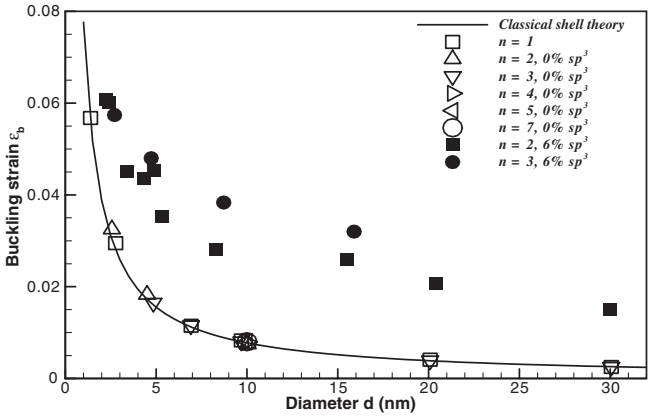

FIG. 2. Buckling strain of SWCNTs and MWCNTs versus average tube diameter. Symbols are MD simulations and the solid line is the classical shell theory result; n is the number of walls.

We computed the interwall shear modulus G as follows. All atoms in the inner wall of a double-walled MWCNT were fixed in the axial direction while an axial force F_a was applied on each atom on the outer wall. This is equivalent to applying uniform shear traction $\tau = NF_a/(\pi dL)$, where N is the number of atoms on the outermost wall. The system was relaxed via MD. We then measured the induced average axial displacement Δ of the outer wall and computed the interwall shear strain as $\gamma = \Delta/\delta$, where δ is the interwall spacing, and the effective shear modulus as $G = \tau/\gamma$. G scales nearly linearly with sp^3 bond fraction as $G \approx f \times (880\ \text{GPa})$ because we are measuring an average property around the entire tube and the sp^3 bond density is low. G is also independent of the nanotube radius. This is the first main result of this Letter.

We computed the compressive deformation and critical buckling strain as follows. All atoms in the first four rings at the bottom of the MWCNT were held fixed in the tube-axis direction while the four rings of atoms at the top of the nanotube were displaced downward rigidly in very small displacement increments (<0.02 Å). After each displacement increment, the structure was relaxed for 2 ps, achieving near equilibrium, and the force was measured. The critical buckling strain corresponds to the point of the first drop in force with increasing compressive strain. Buckling was first simulated for SWCNTs and for MWCNTs with no sp^3 bonds, i.e., only van der Waals coupling, for MWCNTs having *average* diameters ranging from 1 to 50 nm and with up to $n = 7$ walls. These calculations significantly extend those of Yakobson *et al.* [11] and other molecular mechanics results [12]. Figure 2 shows the critical buckling strain versus diameter and the results agree with the classical shell-buckling theory [13] employed for SWCNTs [11] and later extended to MWCNTs [14], depending only on the average radius and not the number of walls. In the presence of interwall coupling via sp^3 bonding, Fig. 2 shows that the buckling strain at any diameter increases notably and also depends on the number of walls and the degree of sp^3 bonding. For all nanotube diameters, shear coupling increases the buckling strain. For the same fraction of sp^3 bonds and mean diameter, the buckling strain increases with the number of walls. Therefore, interwall coupling quantitatively and qualitatively changes the nature of the deformation and improves failure resistance relative to MWCNTs with only van der Waals coupling. This is the second main result of this Letter.

To understand the influence of sp^3 interwall bonding on the buckling strain and to capture it within a continuum framework, we have developed a shear-coupled-shell (SCS) model for an n-walled MWCNT. Under a uniform compressive strain ε_0, let the axial and radial displacements of the walls be perturbed by $u' = A\cos(m\pi x/L)$ and $w' = B\sin(m\pi x/L)$, respectively, where x is the axial coordinate and m is the buckling mode. Such a perturbation necessitates relative sliding of $\delta dw'/dx$ between neighboring walls, resulting in interwall shear stress $\tau = Gdw'/dx$ and a total interwall sliding energy $U_s = (n-1)G\delta m^2\pi^3 RA^2/2L$, where R is the mean radius of the MWCNT. This energy is added to the membrane energy,

$$U_m = \frac{nEh\pi RL}{(1-\nu^2)}(1-\nu^2)\varepsilon_o^2 + \frac{A^2m^2\pi^2}{2L^2} + \frac{B^2}{2R^2} + \frac{\nu m\pi}{RL}AB + \frac{2(1-\nu^2)\varepsilon_o m\pi}{L^2}A\int_0^L \sin(m\pi x/L)dx, \quad (1)$$

the bending energy $U_b = nDm^4\pi^5 RB^2/2L^3$ due to local wall curvature, where $D = Eh^3/12(1-\nu^2)$ is the bending modulus, and the work done by the external compressive force

$$V = -2n\pi REh\varepsilon_o^2 L - \frac{n}{2L}\pi^3 EhR\varepsilon_o m^2 B^2 - 2n\pi REh\varepsilon_o \frac{m\pi}{L}A\int_0^L \sin(m\pi x/L)dx \quad (2)$$

to obtain the total potential energy $\Pi = U_m + U_b + U_s + V$. Minimizing Π with respect to the perturbation amplitudes A and B, enforcing existence of nontrivial A and B, and finally minimizing with respect to m gives the critical

buckling strain ε_b as

$$\varepsilon_b = \frac{h}{R\sqrt{3(1-\nu^2)}} + \frac{n-1}{n}\frac{G\delta}{Eh} \tag{3}$$

Further details of the SCS model can be found in the supplementary document [15]. The first term on the right-hand side of Eq. (3) is the standard shell theory result [11,13,14] which is recovered in the absence of sp^3 interwall bonding ($G \to 0$). The second term is due to interwall shear coupling, which resists interwall sliding and increases the stability of the structure.

Figure 3 shows a normalized buckling strain versus interwall coupling for several MD simulations and for the SCS model. In Fig. 3, the interwall coupling is represented by the nondimensional quantity $\eta = E_g/G(1-\nu^2)$, where E_g is the in-plane Young's modulus of a graphite sheet, and the buckling strain ε_b is normalized as $\xi(\varepsilon_b/\varepsilon_c - 1)$ with $\xi = (\frac{n}{n-1})(\frac{E}{E_g})(\frac{h^2}{R\delta})\sqrt{\frac{1-\nu^2}{3}}$. As a result, the normalized SCS buckling strain is a function of η only. Figure 3 shows that as $G \to 0$ ($\eta \to \infty$), the MD and SCS results agree and converge to the classical shell theory result. As G increases (η decreases), the buckling strain also increases significantly and the SCS model agrees very well with the MD results over more than 2 orders of magnitude change in η. Figure 4 shows the SCS model prediction for the buckling strains against actual MD values for all cases simulated. Perfect agreement would correspond to all data points lying on the dashed line of slope unity. The SCS model is in very good agreement with the entire set of MD data points for CNTs with different number of walls, demonstrating that the continuum SCS model captures the essential mechanics of interwall shear-coupled MWCNTs. This is the third main result of this Letter.

As can be seen in Fig. 3, at extremely high percentage of sp^3 bonds ($\eta \to 0$), the SCS model does not recover the isotropic continuum limit due to the assumption of equal stress states in each wall, which is a good approximation for small values of G. The continuum limit can be recovered by modeling the MWCNT as a transversely isotropic shell (TIS) (see supplementary material in Ref. [15]). Figure 3 shows the predictions of the TIS model, which attains the correct continuum limit as $\eta \to 0$ and is reasonably close to the SCS model over a large range of η, but fails in the regime of $\eta \to \infty$, where SCS model continues to work well.

The predictions from our MD simulations and SCS model rationalize experimental results on shell-buckling of individual MWCNT fabricated by chemical vapor deposition technique [16]. It is well known that experimental buckling strains are significantly smaller than the theoretical values because of imperfection sensitivity [17]. However, in the experiments the average critical buckling strain was 2.875×10^{-3} [16], whereas the value for ideal MWCNTs is only 1.725×10^{-3}. Furthermore, Raman spectroscopy analysis on similarly-fabricated MWCNTs shows an sp^3 peak at 1332 cm^{-1} in addition to usual sp^2 peak at 1582 cm^{-1} [18,19]. From the Raman intensity ratio, the sp^3/sp^2 ratio in the experimental samples $\approx$0.1–0.4 [20], equivalent to 1%–6% of interwall sp^3 bonds. Using the measured buckling strain and the SCS model, we estimate the effective shear modulus as $G \sim$ 1.3 GPa corresponding to 0.25% sp^3 bonds. Quantitative agreement is therefore not obtained by a simple analysis. The difference could lie in the imperfection sensitivity: the experimental buckling strain could be the net result of an increase due to shear coupling and a decrease due to imperfections. The SCS model provides an upper bound for the buckling strain in the presence of interwall coupling.

Finally, we have simulated the pullout behavior of inner walls from outer walls in the presence of interwall bonding, complementing our prior work on pullout in van der Waals

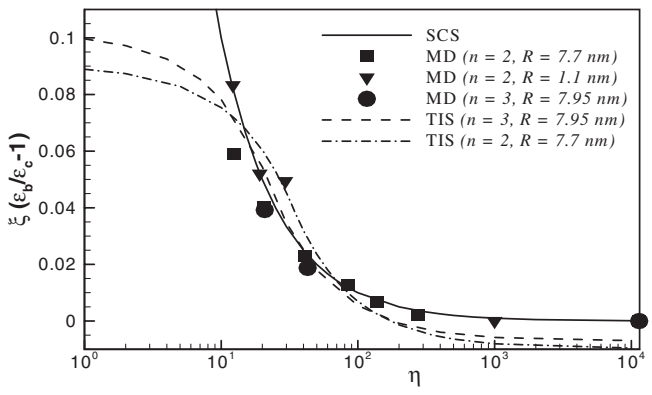

FIG. 3. Buckling strain ε_b of MWCNTs, normalized as $\xi(\varepsilon_b/\varepsilon_c - 1)$, versus the nondimensional interwall shear parameter η, predicted by MD simulation, and SCS and TIS models.

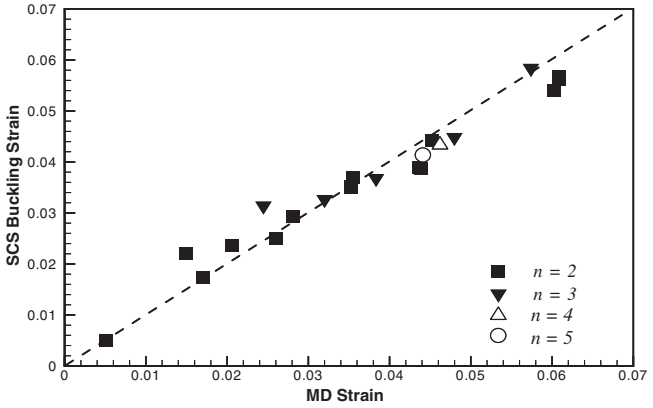

FIG. 4. Buckling strain predicted by the SCS model versus the buckling strain obtained via MD simulations, for a range of MWCNT diameter, percentage of sp^3 bonds, and number of walls.

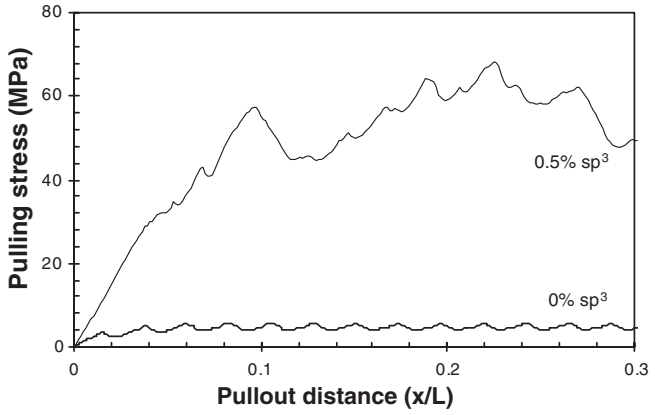

FIG. 5. Pullout force versus pullout distance for double-wall CNTs with 0% and 0.5% sp^3 bonds ($L = 5$ nm).

bonded MWCNTs [3]. Figure 5 shows the results of one simulation of a double-walled nanotube of radius $R =$ 1.2 nm for both 0% sp^3 bonding and 0.5% sp^3 bonding with uncapped ends. The initial pullout force with modest interwall bonding is ≈10 times larger than that of the ideal MWCNT, with a much larger initial range of nearly-elastic behavior as the sp^3 bonds stretch and ultimately fail. After the initial yielding, the ''steady'' pullout force for the nanotubes with sp^3 bonds is governed by the formation of new sp^3 bonds at the end of the nanotube. The details of this mechanism require more investigation. In any case, the interwall bonding provides much greater shear coupling, as noted earlier via the computation of G, and much larger energy absorption capability during the subsequent ''pullout'' phase of the deformation. This is the fourth main result of this Letter.

There is experimental evidence that shear coupling due to sp^3 bonds enhances the toughness of MWCNT-reinforced ceramic composites. In materials nominally identical to those studied in Ref. [16], MWCNT pullout from the matrix on the fractured surface of CNT-alumina composites is observed, but with relatively short lengths and no obvious telescoping within the nanotubes [21]. In nanoindentation testing, MWCNT bridging across crack faces was also clearly seen and was subsequently estimated to increase the composite toughness by up to 10 times the matrix toughness [22].

Most of the past and current research effort on utilizing the excellent mechanical properties of carbon nanotubes has focused on using SWCNTs and MWCNTs as stiffening fibers in polymer and ceramic composite materials. Although such an approach has been promising, so far the gains in strength and toughness of such composites has been modest, possibly because the inner walls do not fully participate in the loading process. The results presented here demonstrate that the superior of mechanical properties of MWCNTs can be realized by controlling interwall coupling, number of walls and radius. Specifically, interwall coupling and the associated enhanced interwall shear resistance mitigate three major problems with ideal MWCNTs by increasing (i) the interwall load transfer, (ii) the critical buckling strain, and (iii) the fiber pullout, solving the telescoping problem and enhancing energy dissipation. The simulation and analytical results here thus provide the basis for an engineering design strategy for high mechanical performance in MWCNT-based systems.

Z. X. and W. C. gratefully acknowledge support of this work by the US AFOSR through Grant No. FA9550-04-1-0402 and by the NSF through the NIRT program No. CMS-0304246. P. R. G. gratefully acknowledges the support from the AFOSR (Grant No. FA9550-05-1-0210).

[1] M. F. Yu *et al.*, Science **287**, 637 (2000).
[2] B. I. Yakobson and P. Avouris, Top. Appl. Phys. **80**, 287 (2001).
[3] Z. Xia and W. A. Curtin, Phys. Rev. B **69**, 233408 (2004).
[4] J. Seldin and C. W. Nezbeda, J. Appl. Phys. **41**, 3389 (1970).
[5] T. Tanabe, Phys. Scr. **T64**, 7 (1996).
[6] E. Salonen, A. V. Krasheninnikov, and K. Nordlund, Nucl. Instrum. Methods Phys. Res., Sect. B **193**, 603 (2002).
[7] A. Kis *et al.*, Nat. Mater. **3**, 153 (2004).
[8] M. Huhtala *et al.*, Phys. Rev. B **70**, 045404 (2004).
[9] D. W. Brenner, Phys. Rev. B **42**, 9458 (1990).
[10] Z. Mao, A. Garg and S. B. Sinnott, Nanotechnology **10**, 273 (1999).
[11] B. I. Yakobson, C. J. Brabec, and J. Bernholc, Phys. Rev. Lett. **76**, 2511 (1996).
[12] A. Searsand and R. C. Batra, Phys. Rev. B **73**, 085410 (2006); C. Li and T.-W. Chou, Mech. Mater. **36**, 1047 (2004).
[13] S. P. Timoshenko and J. M. Gere, *Theory of Elastic Stability* (McGraw-Hill, New York, 1961).
[14] C. Q. Ru, J. Appl. Phys. **89**, 3426 (2001).
[15] See EPAPS Document No. E-PRLTAO-98-012724 for supplementary material: SCS and TIS models. For more information on EPAPS, see http://www.aip.org/pubservs/epaps.html.
[16] J. F. Waters *et al.*, Appl. Phys. Lett. **87**, 103109 (2005).
[17] J. Singer, J. Arbocz, and T. Weller, *Buckling Experiments: Experimental Methods in Buckling of Thin-Walled Structures* (John Wiley & Sons, New York, 2002), Vol. 2.
[18] J. Li, C. Papadopoulos, J. M. Xu, and M. Moskovits, Appl. Phys. Lett. **75**, 367 (1999).
[19] A. Z. Hartman, M. Jouzi, R. L. Barnett, and J. M. Xu, Phys. Rev. Lett. **92**, 236804 (2004).
[20] G. Irmer and A. Dorner-Reisel, Adv. Eng. Mater. **7**, 694 (2005).
[21] Z. H. Xia *et al.*, Acta Mater. **52**, 931 (2004).
[22] Z. H. Xia, W. A. Curtin, and B. W. Sheldon, J. Eng. Mater. Technol. **126**, 238 (2004).